International Journal of Scientific Research in Physics and Applied Sciences
Vol.9, Issue.3, pp.15-20, June (2021)

Research Paper

E-ISSN: 2348-3423

Effect of Inter-dot Coupling on Transmission Probability of a Triple Quantum Dot Systems

S. Chand[1*], S. Devi[2]

[1]University Institute of Technology, Himachal Pradesh University Shimla, HP, India
[2]Department of Physics, Himachal Pradesh University Shimla, HP, India

[*]*Corresponding Author: shyam_hpu@yahoo.co.in Tel.: +91 9816233027*

Available online at: www.isroset.org

Received: 15/Apr/2021, Accepted: 20/May/2021, Online: 30/Jun/2021

***Abstract*—** Following the techniques of non-equilibrium Green function theory for quantum transport, the transmission probability for the electron transport process through the system of linear triple quantum dots arranged in series and parallel geometry has been investigated in the presence of Coulombic interaction. The mean field approximation technique has been applied to decouple the higher order Green functions, which contain Coulomb interaction in their equations of motion. The Green functions so obtained have been incorporated in the derivations for the electron transmission coefficient. The transmission coefficient has been calculated numerically and the role of inter-dot tunneling rate in the behavior of transmission coefficient has been investigated. In series case, the signatures of merging of three dots to form a single big dot become visible in the transmission peak when inter-dot tunneling exceeds lead-dot coupling strength. Whereas, in the parallel configuration, the transmission probability peaks display the clear signs of Fano peaks when inter-dot tunneling is turned on, which indicates the inter-dot tunneling induced Fano interference occurring during the electron transport**.**

Keywords*—Coulomb Blockade Regime, Quantum Dot, Triple Quantum Dot System, Transmission Probability, Fano Effect*

I. INTRODUCTION

Among the low dimensional quantum systems, the quantum dots (QDs) are known to be the smallest man-made solid state nano-systems having discrete energy levels and atomic like properties, hence regarded as artificial atoms [1]. The Electronic transport process in quantum dot (QD) systems had been an area of enormous research interest during the past three decades [2,3,4]. It is possible to fabricate nano-structures with two or more QDs weakly coupled with each other by inter-dot tunnel barriers, which may exhibit molecular like states. The phenomena of electronic transport via single QD and double QD systems, has been explored extensively during past three decades [5,6]. Whereas, the theoretical studies related to the transport through triple quantum dot (TQD) structures have not been carried out in past as much as through the single and double QD system. But, in recent years, the linear arrays of dots with more than two QDs have attracted significant research attention. The novel applications of QD systems are anticipated in the field of quantum computing and QD solar cells [7,8,9,10,11]. Hence, it is increasingly important to explore the spectral and electron transport phenomena in the QD systems which involve more than two dots placed in between the leads.

In recent years, few theoretical attempts were made to investigate transport through TQD systems [12]. But, the scope was limited to the non-interacting regime. But, as far as we know, no theoretical investigation, related to the electron transport through TQD system, takes Coulomb interaction into consideration. This motivates us to theoretically investigate the electron transmission through TQD system in Coulomb blockade regime, where a strong Coulomb correlation influences the electron flow through the system.

The system under investigation is a linear array of three QDs, which we refer to as TQD system. These QDs are tunnel coupled with each other with inter-dot coupling strength V_d and with two leads (having different electron chemical potentials) with lead-dot coupling strength $\Gamma^{L(R)}$. The difference in their electron chemical potentials leads to the flow of electrons from one lead to another via TQD system. The leads are of macroscopic size, having band like spectrum; whereas, QDs are having discrete spectrum. Therefore, the flow of electron through TQD system is typically a resonant tunneling process involving quantum transport phenomena. Experimentally, all the essential parameters like Fermi level of QDs, inter-dot coupling and coupling QDs with leads can be controlled externally.

© 2021, IJSRPAS All Rights Reserved

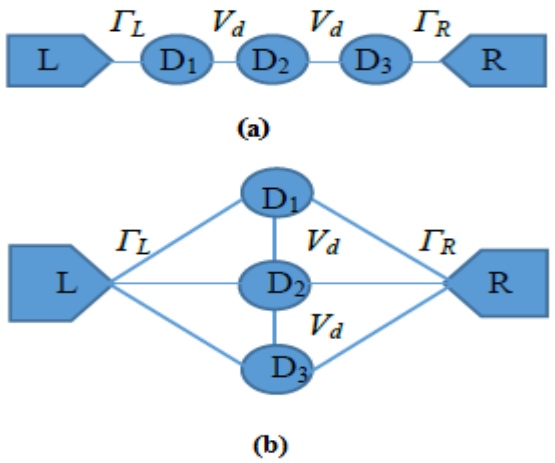

Figure. 1. A typical TQD system in (a) series (b) parallel configuration. Three QDs are weakly tunnel coupled to left (right) lead with coupling strength $\Gamma^{L(R)}$ and with each other with inter-dot coupling V_d.

For completeness, we intend to work on both, series and parallel configurations of linear TQD systems (Fig. 1), in the presence of on-dot Coulomb interaction. We have made use of theory of non-equilibrium Green function (NEGF) formalism [13]. We have derived the QD Green functions (GFs) analytically with the help of equation of motion (EOM) method [14]. Further, we have presented the expression for the electron transmission coefficient in terms of these GFs. In numerical calculations, the electron transmission coefficient has been represented graphically. To present the effect of inter-dot coupling, we tune the value of V_d over a wide range. The results show the merger of three QDs in series case for strong inter-dot coupling and clear signatures of Fano peaks in the plots of transmission probability for parallel case, revealing the occurrence of Fano effect in the given parallel TQD configuration.

Remaining part of the paper discusses the following: Section-II discusses the structure of model Hamiltonian for both series and parallel topologies of TQDs, followed by the analytical results of derivations for QD Green functions in Section-III. The expression for transmission probability has been derived in Section-IV and numerical results have been discussed in Section-V. A briefing of conclusions has been presented in the Section-VI.

II. MODEL HAMILTONIAN FOR A TQD

It is customary to make use of the Anderson model to setup a theoretical model for a typical QD system attached to leads [15,16]. The model Hamiltonian for a TQD system shall have three components such that total Hamiltonian can be written as:

$$H = H_{Leads} + H_{Dots} + H_{Tunneling} \quad (1)$$

For a TQD systems shown in Fig. 1 [(a) and (b)], the model Hamiltonian in expanded form can be written as:

(a) Series configuration:

$$H = \sum_{k\sigma}\varepsilon_k^L\, a_{k\sigma}^\dagger a_{k\sigma} + \sum_{p\sigma}\varepsilon_p^R\; b_{p\sigma}^\dagger b_{p\sigma} + \sum_{i\sigma}\varepsilon_i c_{i\sigma}^\dagger c_{i\sigma} + \sum_i U_i n_{i\uparrow} n_{i\downarrow} + \left[\Sigma_{k\sigma} V_k^L c_{1\sigma}^\dagger a_{k\sigma} + \Sigma_{p\sigma} V_p^R c_{3\sigma}^\dagger b_{p\sigma} + \Sigma_\sigma V_d\,(c_{1\sigma}^\dagger c_{2\sigma} + c_{2\sigma}^\dagger c_{3\sigma}) + H.C.\right] \quad (2)$$

(b) Parallel configuration:

$$H = \sum_{k\sigma}\varepsilon_k^L\, a_{k\sigma}^\dagger a_{k\sigma} + \sum_{p\sigma}\varepsilon_p^R\; b_{p\sigma}^\dagger b_{p\sigma} + \sum_{i\sigma}\varepsilon_i c_{i\sigma}^\dagger c_{i\sigma} + \sum_i U_i n_{i\uparrow} n_{i\downarrow} + \left[\sum_{k\sigma i} V_{ki}^L c_{i\sigma}^\dagger a_{k\sigma} + \sum_{p\sigma i} V_{pi}^R c_{i\sigma}^\dagger b_{p\sigma} + \Sigma_\sigma V_d\,(c_{1\sigma}^\dagger c_{2\sigma} + c_{2\sigma}^\dagger c_{3\sigma}) + H.C.\right] \quad (3)$$

In the above expressions, $\varepsilon_{k(P)}^{L(R)}$ are thermal kinetic energies of non-interacting free electrons contained in left (right) lead exhibiting band, $a_{k\sigma}^\dagger(a_{k\sigma})$ and $b_{p\sigma}^\dagger(b_{p\sigma})$ are the creation (annihilation) operators for the electrons in left (right) leads. The ε_i is the energy of electron in the discrete energy level on i^{th} dot, $c_{i\sigma}^\dagger(c_{i\sigma})$ are electron creation (annihilation) operators on dots. The factor U_i is the on-dot Coulomb interaction for electrons on i^{th} dot, having value relative to other parameter such that dots are in Coulomb blockade regime. The $n_{i\sigma} = c_{i\sigma}^\dagger c_{i\sigma}$ represents the occupation number for electron. Further, $V_{k(p)i}^{L(R)}$ is the coupling potential of left (right) tunnel barriers with i^{th} dot which are essentially the tunneling matrix. Furthermore, the parameter V_d is inter-dot tunneling potential.

III. GREEN FUNCTIONS OF QDS

Since, QD systems are nano-scale structures; hence, the electron transport through QDs is typically a quantum transport and is essentially a many body non-equilibrium problem. The common trend to study such a transport has been to make use of non-equilibrium Green Function (NEGF) approach, as the latter has been the most effective theoretical method to investigate electron transport process in QD systems [17]. As far as NEGF formalism is concerned, three Green functions (GFs) find their applications explicitly in quantum transport, namely retarded GF (G^r), advanced GF (G^a) and lesser than GF ($G^<$). The fundamentals of these GFs such as definitions and properties are found mostly in the literature dealing with many body problems in condensed matter physics [18,19,20,21].

The calculations of these three GFs involve equation of motion (EOM) method [14]. To make the presentation of calculations as brief as possible, the derivations of retarded GFs of QDs have been presented because the analytical calculations of the other GFs also follow the same procedure. In case of a TQD system, the retarded GF matrix has the following shape:

$$G^r = \begin{bmatrix} G_{11}^r & G_{12}^r & G_{13}^r \\ G_{21}^r & G_{22}^r & G_{23}^r \\ G_{31}^r & G_{32}^r & G_{33}^r \end{bmatrix} \quad (4)$$

© 2021, IJSRPAS All Rights Reserved

Here, the various matrix elements represent the retarded GFs of triple QD system defined as: $G_{ij}^{r} = \langle\langle c_{i\sigma}, c_{j\sigma}^{\dagger}\rangle\rangle^{r}$, with i, j =1, 2, 3. Now, we need to get the expressions for these GFs for series and parallel configurations of QDs separately with the help of corresponding Hamiltonian, using EOM method.

(a) Series Configuration

The EOMs for various GFs (Fourier transformed) of QDs in series configuration give following equations:

$$\omega\langle\langle c_{1\sigma}, c_{1\sigma}^{\dagger}\rangle\rangle_{\omega}^{r} = 1 + \varepsilon_1\langle\langle c_{1\sigma}, c_{1\sigma}^{\dagger}\rangle\rangle_{\omega}^{r} + \mathrm{V_d}\langle\langle c_{2\sigma}, c_{1\sigma}^{\dagger}\rangle\rangle_{\omega}^{r} + V_k^{L}\langle\langle a_{k\sigma}, c_{1\sigma}^{\dagger}\rangle\rangle_{\omega}^{r} + U_1\langle\langle c_{1\sigma}n_{1-\sigma}, c_{1\sigma}^{\dagger}\rangle\rangle_{\omega}^{r} \quad (5)$$

$$\omega\langle\langle c_{2\sigma}, c_{2\sigma}^{\dagger}\rangle\rangle_{\omega}^{r} = 1 + \varepsilon_2\langle\langle c_{2\sigma}, c_{2\sigma}^{\dagger}\rangle\rangle_{\omega}^{r} + V_d^{*}\langle\langle c_{1\sigma}, c_{2\sigma}^{\dagger}\rangle\rangle_{\omega}^{r} + \mathrm{V_d}\langle\langle c_{3\sigma}, c_{2\sigma}^{\dagger}\rangle\rangle_{\omega}^{r} + U_2\langle\langle c_{2\sigma}n_{2-\sigma}, c_{2\sigma}^{\dagger}\rangle\rangle_{\omega}^{r} \quad (6)$$

$$\omega\langle\langle c_{3\sigma}, c_{3\sigma}^{\dagger}\rangle\rangle_{\omega}^{r} = 1 + \varepsilon_3\langle\langle c_{3\sigma}, c_{3\sigma}^{\dagger}\rangle\rangle_{\omega}^{r} + V_d^{*}\langle\langle c_{2\sigma}, c_{3\sigma}^{\dagger}\rangle\rangle_{\omega}^{r} + V_p^{R}\langle\langle b_{p\sigma}, c_{3\sigma}^{\dagger}\rangle\rangle_{\omega}^{r} + U_3\langle\langle c_{3\sigma}n_{3-\sigma}, c_{3\sigma}^{\dagger}\rangle\rangle_{\omega}^{r} \quad (7)$$

$$\omega\langle\langle c_{1\sigma}, c_{2\sigma}^{\dagger}\rangle\rangle_{\omega}^{r} = \varepsilon_1\langle\langle c_{1\sigma}, c_{2\sigma}^{\dagger}\rangle\rangle_{\omega}^{r} + \mathrm{V_d}\langle\langle c_{2\sigma}, c_{2\sigma}^{\dagger}\rangle\rangle_{\omega}^{r} + V_k^{L}\langle\langle a_{k\sigma}, c_{1\sigma}^{\dagger}\rangle\rangle_{\omega}^{r} + U_1\langle\langle c_{1\sigma}n_{1-\sigma}, c_{2\sigma}^{\dagger}\rangle\rangle_{\omega}^{r} \quad (8)$$

$$\omega\langle\langle c_{3\sigma}, c_{1\sigma}^{\dagger}\rangle\rangle_{\omega}^{r} = \varepsilon_3\langle\langle c_{3\sigma}, c_{1\sigma}^{\dagger}\rangle\rangle_{\omega}^{r} + V_d^{*}\langle\langle c_{2\sigma}, c_{1\sigma}^{\dagger}\rangle\rangle_{\omega}^{r} + V_p^{R}\langle\langle b_{p\sigma}, c_{1\sigma}^{\dagger}\rangle\rangle_{\omega}^{r} + U_3\langle\langle c_{3\sigma}n_{3-\sigma}, c_{1\sigma}^{\dagger}\rangle\rangle_{\omega}^{r} \quad (9)$$

$$\omega\langle\langle c_{1\sigma}, c_{3\sigma}^{\dagger}\rangle\rangle_{\omega}^{r} = \varepsilon_1\langle\langle c_{1\sigma}, c_{3\sigma}^{\dagger}\rangle\rangle_{\omega}^{r} + \mathrm{V_d}\langle\langle c_{2\sigma}, c_{3\sigma}^{\dagger}\rangle\rangle_{\omega}^{r} + V_k^{L}\langle\langle a_{k\sigma}, c_{3\sigma}^{\dagger}\rangle\rangle_{\omega}^{r} + U_1\langle\langle c_{1\sigma}n_{1-\sigma}, c_{3\sigma}^{\dagger}\rangle\rangle_{\omega}^{r} \quad (10)$$

$$\omega\langle\langle c_{2\sigma}, c_{1\sigma}^{\dagger}\rangle\rangle_{\omega}^{r} = \varepsilon_2\langle\langle c_{2\sigma}, c_{1\sigma}^{\dagger}\rangle\rangle_{\omega}^{r} + V_d^{*}\langle\langle c_{2\sigma}, c_{1\sigma}^{\dagger}\rangle\rangle_{\omega}^{r} + U_2\langle\langle c_{2\sigma}n_{2-\sigma}, c_{1\sigma}^{\dagger}\rangle\rangle_{\omega}^{r} \quad (11)$$

$$\omega\langle\langle c_{2\sigma}, c_{3\sigma}^{\dagger}\rangle\rangle_{\omega}^{r} = \varepsilon_2\langle\langle c_{2\sigma}, c_{3\sigma}^{\dagger}\rangle\rangle_{\omega}^{r} + V_d^{*}\langle\langle c_{2\sigma}, c_{3\sigma}^{\dagger}\rangle\rangle_{\omega}^{r} + U_2\langle\langle c_{2\sigma}n_{2-\sigma}, c_{3\sigma}^{\dagger}\rangle\rangle_{\omega}^{r} \quad (12)$$

$$\omega\langle\langle c_{3\sigma}, c_{2\sigma}^{\dagger}\rangle\rangle_{\omega}^{r} = \varepsilon_3\langle\langle c_{3\sigma}, c_{2\sigma}^{\dagger}\rangle\rangle_{\omega}^{r} + V_d^{*}\langle\langle c_{2\sigma}, c_{2\sigma}^{\dagger}\rangle\rangle_{\omega}^{r} + V_p^{R}\langle\langle b_{p\sigma}, c_{2\sigma}^{\dagger}\rangle\rangle_{\omega}^{r} + U_3\langle\langle c_{3\sigma}n_{3-\sigma}, c_{2\sigma}^{\dagger}\rangle\rangle_{\omega}^{r} \quad (13)$$

The EOMs of new GFs, appearing on the RHS of above equations due to lead-dot coupling, result into following Dyson equations:

$$\langle\langle a_{k\sigma}, c_{1\sigma}^{\dagger}\rangle\rangle_{\omega}^{r} = V_k^{L}g_k^{r}\langle\langle c_{1\sigma}, c_{1\sigma}^{\dagger}\rangle\rangle_{\omega}^{r} \quad (14)$$

$$\langle\langle b_{p\sigma}, c_{3\sigma}^{\dagger}\rangle\rangle_{\omega}^{r} = V_p^{R}g_p^{r}\langle\langle c_{3\sigma}, c_{3\sigma}^{\dagger}\rangle\rangle_{\omega}^{r} \quad (15)$$

(b) Parallel Configuration

Similarly, the EOMs of various GFs of QDs in parallel configuration give following equations:

$$\omega\langle\langle c_{1\sigma}, c_{1\sigma}^{\dagger}\rangle\rangle_{\omega}^{r} = 1 + \varepsilon_1\langle\langle c_{1\sigma}, c_{1\sigma}^{\dagger}\rangle\rangle_{\omega}^{r} + \mathrm{V_d}\langle\langle c_{2\sigma}, c_{1\sigma}^{\dagger}\rangle\rangle_{\omega}^{r} + V_{k1}^{L}\langle\langle a_{k\sigma}, c_{1\sigma}^{\dagger}\rangle\rangle_{\omega}^{r} + V_p^{R}\langle\langle b_{p\sigma}, c_{1\sigma}^{\dagger}\rangle\rangle_{\omega}^{r} + U_1\langle\langle c_{1\sigma}n_{1-\sigma}, c_{1\sigma}^{\dagger}\rangle\rangle_{\omega}^{r} \quad (16)$$

$$\omega\langle\langle c_{1\sigma}, c_{2\sigma}^{\dagger}\rangle\rangle_{\omega}^{r} = \varepsilon_1\langle\langle c_{1\sigma}, c_{2\sigma}^{\dagger}\rangle\rangle_{\omega}^{r} + \mathrm{V_d}\langle\langle c_{2\sigma}, c_{2\sigma}^{\dagger}\rangle\rangle_{\omega}^{r} + V_{k1}^{L}\langle\langle a_{k\sigma}, c_{2\sigma}^{\dagger}\rangle\rangle_{\omega}^{r} + V_{p1}^{R}\langle\langle b_{p\sigma}, c_{2\sigma}^{\dagger}\rangle\rangle_{\omega}^{r} + U_1\langle\langle c_{1\sigma}n_{1-\sigma}, c_{2\sigma}^{\dagger}\rangle\rangle_{\omega}^{r} \quad (17)$$

$$\omega\langle\langle c_{1\sigma}, c_{3\sigma}^{\dagger}\rangle\rangle_{\omega}^{r} = \varepsilon_1\langle\langle c_{1\sigma}, c_{3\sigma}^{\dagger}\rangle\rangle_{\omega}^{r} + \mathrm{V_d}\langle\langle c_{2\sigma}, c_{3\sigma}^{\dagger}\rangle\rangle_{\omega}^{r} + V_{k1}^{L}\langle\langle a_{k\sigma}, c_{3\sigma}^{\dagger}\rangle\rangle_{\omega}^{r} + V_{p1}^{R}\langle\langle b_{p\sigma}, c_{3\sigma}^{\dagger}\rangle\rangle_{\omega}^{r} + U_1\langle\langle c_{1\sigma}n_{1-\sigma}, c_{3\sigma}^{\dagger}\rangle\rangle_{\omega}^{r} \quad (18)$$

$$\omega\langle\langle c_{3\sigma}, c_{1\sigma}^{\dagger}\rangle\rangle_{\omega}^{r} = \varepsilon_3\langle\langle c_{3\sigma}, c_{1\sigma}^{\dagger}\rangle\rangle_{\omega}^{r} + V_d^{*}\langle\langle c_{2\sigma}, c_{1\sigma}^{\dagger}\rangle\rangle_{\omega}^{r} + V_{k3}^{L}\langle\langle a_{k\sigma}, c_{1\sigma}^{\dagger}\rangle\rangle_{\omega}^{r} + V_{p3}^{R}\langle\langle b_{p\sigma}, c_{1\sigma}^{\dagger}\rangle\rangle_{\omega}^{r} + U_3\langle\langle c_{3\sigma}n_{3-\sigma}, c_{1\sigma}^{\dagger}\rangle\rangle_{\omega}^{r} \quad (19)$$

$$\omega\langle\langle c_{3\sigma}, c_{2\sigma}^{\dagger}\rangle\rangle_{\omega}^{r} = \varepsilon_3\langle\langle c_{3\sigma}, c_{2\sigma}^{\dagger}\rangle\rangle_{\omega}^{r} + V_d^{*}\langle\langle c_{2\sigma}, c_{2\sigma}^{\dagger}\rangle\rangle_{\omega}^{r} + V_{k3}^{L}\langle\langle a_{k\sigma}, c_{2\sigma}^{\dagger}\rangle\rangle_{\omega}^{r} + V_{p3}^{R}\langle\langle b_{p\sigma}, c_{2\sigma}^{\dagger}\rangle\rangle_{\omega}^{r} + U_3\langle\langle c_{3\sigma}n_{3-\sigma}, c_{2\sigma}^{\dagger}\rangle\rangle_{\omega}^{r} \quad (20)$$

$$\omega\langle\langle c_{2\sigma}, c_{2\sigma}^{\dagger}\rangle\rangle_{\omega}^{r} = 1 + \varepsilon_2\langle\langle c_{2\sigma}, c_{2\sigma}^{\dagger}\rangle\rangle_{\omega}^{r} + V_d^{*}\langle\langle c_{1\sigma}, c_{2\sigma}^{\dagger}\rangle\rangle_{\omega}^{r} + \mathrm{V_d}\langle\langle c_{3\sigma}, c_{2\sigma}^{\dagger}\rangle\rangle_{\omega}^{r} + V_{k2}^{L}\langle\langle a_{k\sigma}, c_{2\sigma}^{\dagger}\rangle\rangle_{\omega}^{r} + V_{p2}^{R}\langle\langle b_{p\sigma}, c_{2\sigma}^{\dagger}\rangle\rangle_{\omega}^{r} + U_2\langle\langle c_{2\sigma}n_{2-\sigma}, c_{2\sigma}^{\dagger}\rangle\rangle_{\omega}^{r} \quad (21)$$

$$\omega\langle\langle c_{3\sigma}, c_{3\sigma}^{\dagger}\rangle\rangle_{\omega}^{r} = 1 + \varepsilon_3\langle\langle c_{3\sigma}, c_{3\sigma}^{\dagger}\rangle\rangle_{\omega}^{r} + V_d^{*}\langle\langle c_{2\sigma}, c_{3\sigma}^{\dagger}\rangle\rangle_{\omega}^{r} + V_{k3}^{L}\langle\langle a_{k\sigma}, c_{1\sigma}^{\dagger}\rangle\rangle_{\omega}^{r} + V_{p3}^{R}\langle\langle b_{p\sigma}, c_{1\sigma}^{\dagger}\rangle\rangle_{\omega}^{r} + U_3\langle\langle c_{3\sigma}n_{3-\sigma}, c_{3\sigma}^{\dagger}\rangle\rangle_{\omega}^{r} \quad (22)$$

$$\omega\langle\langle c_{2\sigma}, c_{1\sigma}^{\dagger}\rangle\rangle_{\omega}^{r} = \varepsilon_2\langle\langle c_{2\sigma}, c_{1\sigma}^{\dagger}\rangle\rangle_{\omega}^{r} + V_d^{*}\langle\langle c_{1\sigma}, c_{1\sigma}^{\dagger}\rangle\rangle_{\omega}^{r} + \mathrm{V_d}\langle\langle c_{3\sigma}, c_{1\sigma}^{\dagger}\rangle\rangle_{\omega}^{r} + V_{k2}^{L}\langle\langle a_{k\sigma}, c_{1\sigma}^{\dagger}\rangle\rangle_{\omega}^{r} + V_{p2}^{R}\langle\langle b_{p\sigma}, c_{1\sigma}^{\dagger}\rangle\rangle_{\omega}^{r} + U_2\langle\langle c_{2\sigma}n_{2-\sigma}, c_{1\sigma}^{\dagger}\rangle\rangle_{\omega}^{r} \quad (23)$$

$$\omega\langle\langle c_{2\sigma}, c_{3\sigma}^{\dagger}\rangle\rangle_{\omega}^{r} = \varepsilon_2\langle\langle c_{2\sigma}, c_{3\sigma}^{\dagger}\rangle\rangle_{\omega}^{r} + V_d^{*}\langle\langle c_{1\sigma}, c_{3\sigma}^{\dagger}\rangle\rangle_{\omega}^{r} + \mathrm{V_d}\langle\langle c_{3\sigma}, c_{3\sigma}^{\dagger}\rangle\rangle_{\omega}^{r} + V_{k2}^{L}\langle\langle a_{k\sigma}, c_{3\sigma}^{\dagger}\rangle\rangle_{\omega}^{r} + V_{p2}^{R}\langle\langle b_{p\sigma}, c_{3\sigma}^{\dagger}\rangle\rangle_{\omega}^{r} + U_2\langle\langle c_{2\sigma}n_{2-\sigma}, c_{3\sigma}^{\dagger}\rangle\rangle_{\omega}^{r} \quad (24)$$

The EOMs of new GFs, appearing on the RHS of above equations due to lead-dot coupling, result into following Dyson equations:

$$\langle\langle a_{k\sigma}, c_{1\sigma}^{\dagger}\rangle\rangle_{\omega}^{r} = V_{k1}^{L*}g_k^{r}\langle\langle c_{1\sigma}, c_{1\sigma}^{\dagger}\rangle\rangle_{\omega}^{r} + V_{k2}^{L*}g_k^{r}\langle\langle c_{2\sigma}, c_{1\sigma}^{\dagger}\rangle\rangle_{\omega}^{r} + V_{k3}^{L*}g_k^{r}\langle\langle c_{3\sigma}, c_{1\sigma}^{\dagger}\rangle\rangle_{\omega}^{r} \quad (25)$$

$$\langle\langle b_{p\sigma}, c_{1\sigma}^{\dagger}\rangle\rangle_{\omega}^{r} = V_{p1}^{R*}g_p^{r}\langle\langle c_{1\sigma}, c_{1\sigma}^{\dagger}\rangle\rangle_{\omega}^{r} + V_{p2}^{R*}g_p^{r}\langle\langle c_{2\sigma}, c_{1\sigma}^{\dagger}\rangle\rangle_{\omega}^{r} + V_{p3}^{R*}g_p^{r}\langle\langle c_{3\sigma}, c_{1\sigma}^{\dagger}\rangle\rangle_{\omega}^{r} \quad (26)$$

$$\langle\langle a_{k\sigma}, c_{2\sigma}^{\dagger}\rangle\rangle_{\omega}^{r} = V_{k1}^{L*}g_k^{r}\langle\langle c_{1\sigma}, c_{2\sigma}^{\dagger}\rangle\rangle_{\omega}^{r} + V_{k2}^{L*}g_k^{r}\langle\langle c_{2\sigma}, c_{2\sigma}^{\dagger}\rangle\rangle_{\omega}^{r} + V_{k3}^{L*}g_k^{r}\langle\langle c_{3\sigma}, c_{2\sigma}^{\dagger}\rangle\rangle_{\omega}^{r} \quad (27)$$

$$\langle\langle b_{p\sigma}, c_{2\sigma}^{\dagger}\rangle\rangle_{\omega}^{r} = V_{p1}^{R*}g_p^{r}\langle\langle c_{1\sigma}, c_{2\sigma}^{\dagger}\rangle\rangle_{\omega}^{r} + V_{p2}^{R*}g_p^{r}\langle\langle c_{2\sigma}, c_{2\sigma}^{\dagger}\rangle\rangle_{\omega}^{r} + V_{p3}^{R*}g_p^{r}\langle\langle c_{3\sigma}, c_{2\sigma}^{\dagger}\rangle\rangle_{\omega}^{r} \quad (28)$$

$$\langle\langle a_{k\sigma}, c_{3\sigma}^{\dagger}\rangle\rangle_{\omega}^{r} = V_{k1}^{L*}g_k^{r}\langle\langle c_{1\sigma}, c_{3\sigma}^{\dagger}\rangle\rangle_{\omega}^{r} + V_{k2}^{L*}g_k^{r}\langle\langle c_{2\sigma}, c_{3\sigma}^{\dagger}\rangle\rangle_{\omega}^{r} + V_{k3}^{L*}g_k^{r}\langle\langle c_{3\sigma}, c_{3\sigma}^{\dagger}\rangle\rangle_{\omega}^{r} \quad (29)$$

$$\langle\langle b_{p\sigma}, c_{3\sigma}^{\dagger}\rangle\rangle_{\omega}^{r} = V_{p1}^{R*}g_p^{r}\langle\langle c_{1\sigma}, c_{3\sigma}^{\dagger}\rangle\rangle_{\omega}^{r} + V_{p2}^{R*}g_p^{r}\langle\langle c_{2\sigma}, c_{3\sigma}^{\dagger}\rangle\rangle_{\omega}^{r} + V_{p3}^{R*}g_p^{r}\langle\langle c_{3\sigma}, c_{3\sigma}^{\dagger}\rangle\rangle_{\omega}^{r} \quad (30)$$

In GFs of the type $U_i\langle\langle c_{i\sigma}n_{i-\sigma}, c_{i\sigma}^{\dagger}\rangle\rangle_{\omega}^{r}$ appearing in some of the above equations originate due to the intra-dot Coulomb interaction term. The EOMs for such types of GFs generate endless chains of higher order GFs, which make closure of GFs impossible unless a suitable

© 2021, IJSRPAS All Rights Reserved

decoupling technique is employed to close the hierarchy [14]. Here, we make use of mean field approximations technique to decouple the higher order GFs [22]. It is important to admit that this decoupling process approximates the effect of Coulomb interaction. When we apply mean field decoupling approximation, GFs of the type $U_i \langle\langle c_{i\sigma} n_{i-\sigma}, c_{i\sigma}^{\dagger} \rangle\rangle_{\omega}^{r}$ reduce to the following shapes:

$$U_i \langle\langle c_{i\sigma} n_{i-\sigma}, c_{i\sigma}^{\dagger} \rangle\rangle_{\omega}^{r} \approx U_i n_{i-\sigma} \langle\langle c_{i\sigma}, c_{i\sigma}^{\dagger} \rangle\rangle_{\omega}^{r} \quad (31)$$

After the use of above approximations and solving all the EOMs simultaneously, all of the retarded GFs of QDs are clearly closed and we can get their final shapes. The final forms of retarded GFs for the dots are given in the matrix form as:

a) GFs of QDs in Series Configuration:

$$G^r = \begin{bmatrix} G_{11}^r & G_{12}^r & G_{13}^r \\ G_{21}^r & G_{22}^r & G_{23}^r \\ G_{31}^r & G_{32}^r & G_{33}^r \end{bmatrix} = \begin{bmatrix} x_1 & -V_{d12} & 0 \\ -V_{d12}^* & x_2 & -V_{d23} \\ 0 & -V_{23}^* & x_3 \end{bmatrix}^{-1} \quad (32)$$

Here,

$$x_1 = \omega - \epsilon_1 - Un_{1-\sigma} + \frac{i}{2}\Gamma_{11}^L$$
$$x_2 = \omega - \epsilon_2 - Un_{2-\sigma}$$
$$x_3 = \omega - \epsilon_3 - Un_{3-\sigma} + \frac{i}{2}\Gamma_{33}^R$$

b) GFs of QDs in Parallel Configuration:

$$G^r = \begin{bmatrix} G_{11}^r & G_{12}^r & G_{13}^r \\ G_{21}^r & G_{22}^r & G_{23}^r \\ G_{31}^r & G_{32}^r & G_{33}^r \end{bmatrix} = \begin{bmatrix} y_1 & Z_{12} & \frac{i}{2}\Gamma_{13} \\ Z_{12}^* & y_2 & Z_{23} \\ \frac{i}{2}\Gamma_{31} & Z_{23}^* & y_3 \end{bmatrix}^{-1} \quad (33)$$

Here,

$$y_1 = \omega - \epsilon_1 - Un_{1-\sigma} + \frac{i}{2}\Gamma_{11}$$
$$y_2 = \omega - \epsilon_2 - Un_{2-\sigma} + \frac{i}{2}\Gamma_{22}$$
$$y_3 = \omega - \epsilon_3 - Un_{3-\sigma} + \frac{i}{2}\Gamma_{33}$$
$$Z_{12} = -V_{d12} + \frac{i}{2}\Gamma_{12}$$
$$Z_{12}^* = -V_{d12}^* + \frac{i}{2}\Gamma_{21}$$
$$Z_{23} = -V_{d23} + \frac{i}{2}\Gamma_{23}$$
$$Z_{23}^* = -V_{d23}^* + \frac{i}{2}\Gamma_{32}$$

In all the above cases, $\Gamma_{ij} = \Gamma_{ij}^L + \Gamma_{ij}^R$ and

$$\Gamma_{ij}^{L(R)} = \sum_{k(p)}^{L(R)} V_{k(p)i(j)}^{L(R)*} V_{k(p)i(j)}^{L(R)} g_{k(p)}^r$$

$= 2\pi \sum_{k(p)}^{L(R)} V_{k(p)}^{L(R)*} V_{k(p)}^{L(R)} \delta\left(\omega - \varepsilon_{k(p)}^{L(R)}\right)$, are the various lead-dot tunnel coupling matrix elements (i, j = 1, 2, 3). In case of the wide-band limit of leads, only the imaginary parts of these couplings are significant. These lead-dot coupling parameters can be represented in the shape of matrices for the series and parallel TQD systems, as follows:

(a) For series TQD

$$\Gamma^L = \begin{bmatrix} \Gamma_{11}^L & 0 & 0 \\ 0 & 0 & 0 \\ 0 & 0 & 0 \end{bmatrix} \text{ and } \Gamma^R = \begin{bmatrix} 0 & 0 & 0 \\ 0 & 0 & 0 \\ 0 & 0 & \Gamma_{33}^R \end{bmatrix}$$

(b) For parallel TQD

$$\Gamma^{L(R)} = \begin{bmatrix} \Gamma_{11}^{L(R)} & \Gamma_{12}^{L(R)} & \Gamma_{13}^{L(R)} \\ \Gamma_{21}^{L(R)} & \Gamma_{22}^{L(R)} & \Gamma_{23}^{L(R)} \\ \Gamma_{31}^{L(R)} & \Gamma_{32}^{L(R)} & \Gamma_{33}^{L(R)} \end{bmatrix}$$

IV. TRANSMISSION COEFFICIENT FOR A TQD SYSTEM

The transmission coefficient of a QD system is contained in the expression of current given by Landauer-Buttiker formula. To obtain the expression for current using NEGF approach, we follow Meir and Wingreen technique, which results into the following Landauer-Buttiker formula [21,23, 24, 25]:

$$I = \frac{e}{h}\sum_{\sigma}\int (f_L - f_R) Tr(G^a \Gamma^R G^r \Gamma^L) d\omega = \frac{e}{h}\sum_{\sigma}\int (f_L - f_R) T(\omega) d\omega \quad (34)$$

In the above equation, $T(\omega)$ is the transmission probability or transmission coefficient and $f_{L(R)}$ is Fermi Dirac distribution function for the electrons in left (right) lead. The transmission coefficient in above equation contains GFs of QDs and is given as:

$$T(\omega) = Tr(G^a \Gamma^R G^r \Gamma^L) \quad (35)$$

Therefore, the final expressions for electronic current and transmission coefficient of the given linear TQD topologies, we can select the corresponding Green function matrices and substitute them in the above equations. Although the shapes of the equations for electronic current and the transmission probability for the different QD systems is the same, yet the form of GFs and the Γ matrices are different for different QD system. So, the final form of transmission coefficient for numerical calculations, after the substitution of various GFs and other matrices, gives us a new result.

V. NUMERICAL RESULTS

In this particular section, the numerical calculations of transmission coefficient for the TQD system, in series and parallel geometry, have been presented. For the sake of simplicity, we may assume that dots have been symmetrically coupled to each other and with the leads.

© 2021, IJSRPAS All Rights Reserved

Experimental observations on such a QD system have shown that the on-dot Coulombic repulsion energy U (U_1=U_2=U_3) is the dominating parameter; therefore, rest of the energies have been expressed in terms of units of U. Also, we assume that three dots are identical in all respect and have same Fermi energy levels with energy i.e. $\varepsilon_1 = \varepsilon_2 = \varepsilon_3 = \varepsilon$ and the same inter-dot coupling V_d. Further, our consideration of a non-magnetic case leads to the averaging of dot level occupation number i.e. $n_{i\sigma} = n_{i-\sigma} = n = \frac{1}{2}$.

In the numerical calculations, we tune the value of inter-dot coupling over a wide range. Experimentally, it becomes possible to vary the different tunnel coupling strengths with the help of the external controls which are the part of fabrication of QD systems. The results presented show the role of inter-dot coupling in deciding the nature of transmission probability spectrum for the TQD system in its series as well as parallel configurations between the two leads. We have tuned the inter-dot tunnel coupling from week coupling regime ($V_d \ll \Gamma$) to strong coupling regime ($V_d \geq \Gamma$).

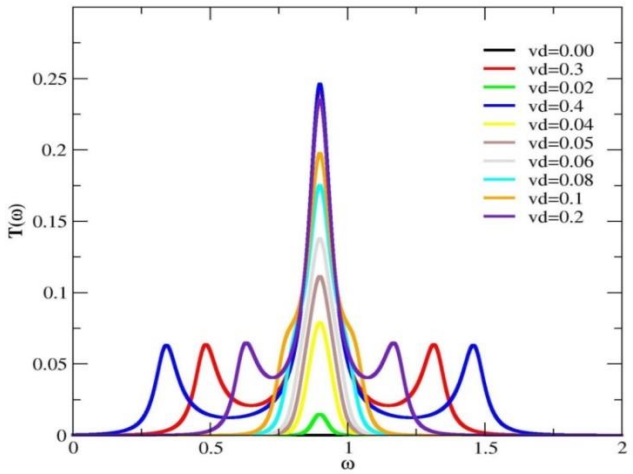

Figure 2. The plot showing transmission coefficient as a function of energy in series configuration of a TQD system with ε = *0.04U*, Γ = *0.08U*, for various values of inter-dot tunneling rate.

The above graph (Fig. 2) shows the transmission coefficient for series configuration of a TQD. Clearly, a single transmission peak appears around energy ε+*0.5U*, due to single resonant level on three identical QDs. Further, we can clearly see the growth in transmission peaks with increase in the tunneling rate parameter or inter-dot coupling V_d increases in weak coupling regime. While at large value of tunneling rate, secondary peaks appear symmetrically about the main transmission peak. This occurs precisely when V_d becomes more than the lead-dot coupling strength Γ i.e. in strong dot-dot coupling regime. The development of secondary peak structure is the clear signs of merging of three QDs to form a single large QD, resulting into renormalization of energy levels around the original resonant level. The occurrence of merger of QDs to form a single bigger dot has previously been observed in case of double QD system also [16], [25].

But, here we have observed the same phenomena for a triple QD system in series and is a new finding for a TQD system. It is important to mention here that the shapes of new renormalized transmission peaks may differ in experimental findings because it is difficult to fabricate the identical QDs, whereas, we have assumed QDs to be identical.

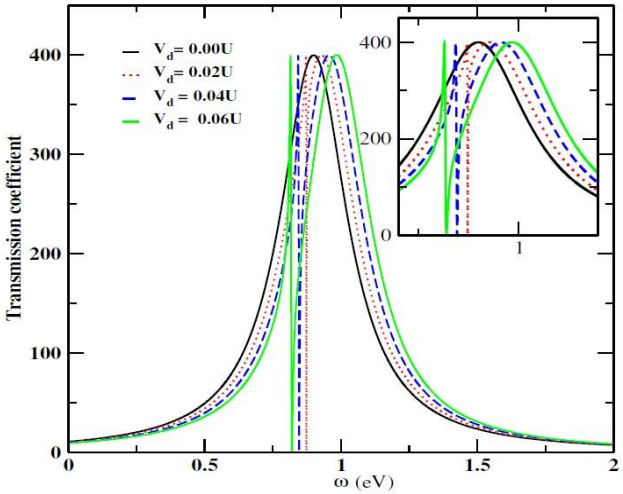

Figure 3. The plot showing transmission coefficient versus energy for parallel configuration of a TQD system with ε = *0.04U*, Γ = *0.08U*, for various values of inter-dot tunneling rate.

Now, let us see the role of inter-dot tunneling here for the case of parallel configuration of TQD system. It is found that V_d. has entirely different effect here. Fig. 3 shows the transmission probability (un-normalized) graphs for parallel configuration of TQD system for different values of V_d. As compared to the series configuration, the transmission probability is quite large in this case due to number of available transmission channels in parallel geometry, whereas, there was only a single transmission channel in series case. When V_d.=*0*, there is a single Lorenzian transmission peak at $\omega = \varepsilon + Un$. As the inter-dot tunneling is introduced (V_d.≠*0*), two types of peak structures appear in transmission spectrum. One of these is a Lorenzian peak appearing around the energy $\omega = \varepsilon + Un$, whereas, another one is a Fano line shaped. The development of Fano resonant peak structure confirms the occurrence of Fano effect in parallel TQD system resulting due to the quantum mechanical interference among the discrete energies of dots and the continuum of energies of electrons in the leads.

The phenomena of Fano effect in QDs, was noticed in double QD system for an asymmetric parallel configuration only [17]. But, Fano peaks always disappear when QDs are arranged in symmetric parallel topology, in the absence of any magnetic flux [25]. However, an important finding of the present theoretical work is the occurrence of Fano effect in symmetric parallel topology for a TQD system, even with no flux threading the system. Furthermore, it is significant to mention here that Fano peak disappears when the inter-dot tunneling is turned off and we observe only the Lorenzian peak in transmission spectrum. Therefore, it can be concluded that the inter-dot

© 2021, IJSRPAS All Rights Reserved

tunneling is responsible for occurrence of Fano effect in a symmetric parallel TQD system.

VI. CONCLUSIONS

In the present work a quantum transport through a linear array of triple quantum dots was investigated in Coulomb blockade regime of transport, using NEGF formalism. The effect of inter-dot tunneling on transmission peak was explored numerically. The following conclusions are drawn from the numerical results presented in the given work:

1. The transmission probability is quite small in series configuration of TQD, as compare to that in parallel configuration.
2. In series TQD system, inter-dot tunneling leads to merger of three QDs to a single big QD in the strong lead dot coupling regime.
3. In parallel TQD system, inter-dot tunneling induces Fano effect even with no magnetic flux.
4. The above observations are important findings of the present work and these observations should be taken into consideration wherever any technological application involves any TQD systems.

REFERENCES

[1] D. Bimberg, M. Grundmann, N. N. Ledentsov, "*Quantum Dot Heterostructures*", Wiley, New York **1999**.

[2] C. A. Stafford and S. Das Sarma, "*Collective Coulomb blockade in an array of quantum dots: A Mott-Hubbard approach*" Phys. Rev. Lett. **Vol.72, pp. 3590-3593, 1994.**

[3] Chang Niu, Li-jun Liu and Tsung-han Lin, "*Coherent transport through a coupled-quantum-dot system with strong intradot interaction*" Phys. Rev. B **Vol.51, pp. 5130-5137, 1995**.

[4] Sushil Lamba and S. K. Joshi, "*Transport through a coupled quantum dot system: Role of interdot interactions*" Phys. Rev. B **Vol. 62, pp. 1580-1583, 2000.**

[5] L. P. Kouwenhoven, D. G. Austin and Tarucha,"*Few-electron quantum dots*" Rep. Prog. Phys. **Vol. 64, pp. 701-736, 2001**.

[6] Shyam Chand, G. Rajput, K. C. Sharma P. K. Ahluwalia,"*Inter-dot coupling effects on transport through correlated parallel coupled quantum dots*" Pramana -Journal of Physics **Vol.72, pp. 887-902, , 2009.**

[7] R. Hanson, L. P. Kouwenhoven, J. R. Petta, S. Tarucha, L. M. K. Vandersypen, "*Spins in few-electron quantum dots*" Rev. Mod. Phys. **Vol.79, pp. 1217-1265, 2007.**

[8] Volk, A. M. J. Zwerver U. Mukhopadhyay, P. T. Eendebak, C. J. van Diepen, J. P. Dehollain, T. Hensgens, T. Fujita, C. Reichl, W.Wegscheider and L. M. K. Vandersypen,"*Loading a quantum-dot based "Qubyte" register*" npj Quantum Information, **pp. 1-8, 2019.**

[9] J. M. Elzerman, R. Hanson, L. H. Willems van Beveren, B. Witkamp, L. M. K. Vandersypen & L. P. Kouwenhoven, "*Single-shot read-out of an individual electron spin in a quantum dot*" Nature **Vol.430, pp. 431–435, 2004**.

[10] .P V Kamat, "*Meeting the Clean Energy Demand: Nanostructure Architectures for Solar Energy Conversion*", J. Phys. Chem. C **Vol.111, pp. 2834-2860, 2007.**

[11] R. K. Das "*Application of Metal Compound Nanomaterials in Quantum Dot Sensitized Solar Cells (QDSSC)*", International Journal of Scientific Research in Physics and Applied Sciences (IJSRPAS), **Vol.5, Issue-5, pp. 16-18, 2017.**

[12] M. L. Ladron de Guevara and P. A. Orellana, "*Quantum transport of electrons through a parallel-coupled triple quantum-dot molecule*" Brazilian Journal of Physics, **Vol. 36, no. 3B, pp. 913-916, 2006.**

[13] A. P. Jauho, N. S. Wingreen, Y. Meir, "*Anderson model out of equilibrium: Noncrossing-approximation approach to transport through a quantum dot*" Phys. Rev. B, **Vol.49, pp. 11040-11052, 1994.**

[14] C. Lacroix, "*Density of states for the Anderson model*" J. Phys. F **Vol.11, pp. 2389-2397, 1981.**

[15] P. W. Anderson, "*Localized Magnetic States in Metals*" Phys. Rev. **Vol.124, pp. 41-60, 1961.**

[16] Sushila Devi, B.B. Brogi, P. K. Ahluwalia, S. Chand, "*Low bias negative differential conductance and reversal of current in coupled quantum dots in different topological configurations*" Physica B **Vol.539, pp. 111-116, 2018**.

[17] Shyam Chand, R. K. Moudgil, P. K. Ahluwalia, "*Fano-effect and negative differential conductance in asymmetric parallel coupled quantum dots*" Physica B **Vol.405, pp. 239-246, 2010**.

[18] L. V. Keldysh, "*Diagram Technique for Nonequilibrium Processes*" Sov. Phys. JETP **Vol.20, pp. 1018-1026, 1965**.

[19] C. Caroli, R. Combescot, P. Nozieres, and D. Saint-James,"*Direct calculation of the tunneling current*" J. Phys. C **Vol.4, pp. 916-929, 1971.**

[20] G. D. Mahan," **Many Particle Physics**", Plenum Press, NY, **2000**.

[21] L. P. Kadanoff and G. Baym, "*Quantum Statistical Mechanics*" Benjamin, New York, **1962**.

[22] M. L. Ladron de Guevara, F. Carlo, P. A. Orellana, "*Ghost Fano resonance in a double quantum dot molecule attached to leads*" Phys. Rev. B **Vol.67, pp. 195335-195340, 2003**.

[23] Gagan Rajput, Rajendra Kumar, Ajay, "*Tunable Josephson effect in hybrid parallel coupled double quantum dot-superconductor tunnel junction*" Superlattices and Microstructures, **Vol.73, pp. 193-202, 2014.**

[24] A. P. Jauho, N. S. Wingreen, Y. Meir, "*Time-dependent transport in interacting and noninteracting resonant-tunneling systems*" Phys. Rev. B **Vol.50, pp. 5528-5544, 1994**.

[25] Bharat B. Brogi, Shyam Chand and P. K. Ahluwalia, "*Phase controlled swapping effect in electron transport through asymmetric parallel coupled quantum dot system*" Physica B **Vol.461, pp. 110-117, 2015**.

[26] F. R. Waugh, M. J. Berry, C. H. Crouch, C. Livermore, D. J. Mar, R. M. Westervelt, K. L. Campman, and A. C. Gossard, "*Measuring interactions between tunnel-coupled quantum dots*" Phys. Rev. B **Vol.53, pp. 1413-1420, 1996.**

AUTHORS PROFILE

Shyam Chand is an Associate Professor and one of the senior Faculty Members at University Institute of Technology, H. P. University Shimla, India. His research field includes theoretical condensed matter physics. He is particularly interested in nano-scale transport theory. He has published more than 20 research papers in reputed journal and has acted as referee for many journals.

Ms. Sushila Devi. is a Faculty Member at one of the colleges affiliated to H. P. University Shimla, India. Recently, Ms. Sushila submitted her Doctoral thesis to H. P. University. Her research area is Theoretical Condensed Matter Physics and has worked on quantum transport through quantum dots and also DFT based simulation tools.

© 2021, IJSRPAS All Rights Reserved